

Two Photon Absorption Properties of 1,3,5-Tricyano-2,4,6-tris(styryl)benzene Derivatives

Bong Rae Cho,^{*,†} Kyung Hwa Son,[†] Sang Hae Lee,[†] Young-Suk Song,[†] Yun-Kyoung Lee,[†] Seung-Joon Jeon,^{*,†} Jun Ho Choi,[‡] Hochan Lee,[‡] and Minhaeng Cho^{*,‡}

Contribution from the Molecular Opto-Electronics Laboratory, Department of Chemistry and Center for Electro- & Photo-Responsive Molecules, Korea University, 1-Anamdong, Seoul 136-701, Korea, and Department of Chemistry and Center for Multidimensional Spectroscopy, School of Chemistry and Molecular Engineering, Korea University, Seoul 136-701, Korea

Received March 23, 2001

Abstract: Two-photon absorption (TPA) properties of 1,3,5-tricyano-2,4,6-tris(styryl)benzene derivatives have been investigated. Comparison of the absorption and fluorescence spectra reveals that these compounds show large Stokes shifts, which increase gradually as the conjugation length increases. One-photon absorption and excitation spectra are similar except that the latter exhibit several peaks near λ_{\max} . It is also found that the one- and two-photon-induced fluorescence excitation spectra are quite similar, which indicates that the one- and two-photon allowed-excited states are the same. The peak TPA cross section values (δ_{\max}) measured with nanosecond pulses by the two-photon-induced fluorescence method are in the range $(50\text{--}2620) \times 10^{-50} \text{ cm}^4 \text{ s/photon}$. The δ_{\max} value increases as the donor strength and conjugation length increase. A linear relationship is observed between δ_{\max} and β , and this $\delta\text{--}\beta$ relationship is found to serve as a useful synthetic strategy for the design of novel TPA dyes with the octupolar structure.

1. Introduction

Synthesis of highly active organic two-photon materials is of considerable interest because of potential applications in three-dimensional optical storage,^{1–3} two-photon fluorescence excitation microscopy,^{4–8} two-photon optical power limiting,^{9–11} two-photon upconverted lasing,^{12,13} and photodynamic therapy.¹⁴ Various design strategies have been employed to synthesize organic molecules with large two-photon absorption

cross sections. Reinhardt et al. synthesized a variety of donor–bridge–acceptor (D– π –A) and donor–bridge–donor (D– π –D) derivatives, in which fluorene, biphenyl, or naphthyl groups are employed as the mobile π -electron bridge, and showed that the TPA cross sections become large if a planar fluorene is used as the π -center.¹⁵ The TPA property of fluorene derivatives was subsequently optimized by Belfield by introducing a variety of donors and acceptors.¹⁶ The important role of the π -center for the design of large TPA dyes was demonstrated by Prasad et al., who showed that the TPA cross section of the D– π –D chromophores based on dithienothiophene as the π -center are larger by an order of magnitude than those of the fluorene derivatives.¹⁷ By combining synthesis, characterization, and theory, Marder, Perry, and Webb found that bis(styryl)-benzene derivatives with donor–acceptor–donor (D–A–D) and acceptor–donor–acceptor (A–D–A) structural motifs, which are linear quadrupolar molecules, show exceptionally large TPA cross sections. Also, increases of the donor strength and the conjugation length resulted in the increased TPA cross section.¹⁸ Our theoretical calculations also strongly support their observations.¹⁹

In contrast to the extensive investigation on the structure–TPA relationship of the dipolar and quadrupolar molecules, there is only one report on the TPA property of the octupolar molecule. Prasad and co-workers showed that multibranching structure significantly increases the TPA cross section in comparison to the singly branched counterpart,²⁰ whereas no

[†] Molecular Opto-Electronics Laboratory, Department of Chemistry and Center for Electro- & Photo-Responsive Molecules.

[‡] Department of Chemistry and Center for Multidimensional Spectroscopy, School of Chemistry and Molecular Engineering.

(1) Parthenopoulos, D. A.; Rentzepis, P. M. *Science* **1989**, *245*, 843.

(2) Dvornikov, A. S.; Rentzepis, P. M. W. *Opt. Commun.* **1995**, *119*, 341.

(3) Cumpston, B. H.; Ananthavel, S. P.; Barlow, S.; Dyer, D. L.; Ehrlich, J. E.; Erskine, L. L.; Heikal, A. A.; Kuebler, S. M.; Lee, I.-Y. S.; McCord-Maughon, D.; Qin, J.; Röckel, H.; Rumi, M.; Wu, X.-L.; Marder, S. R.; Perry, J. W. *Nature* **1999**, *398*, 51.

(4) (a) Denk, W.; Strickler, J. H.; Webb, W. W. *Science* **1990**, *248*, 73.

(b) Mertz, J.; Xu, C.; Webb, W. W. *Opt. Lett.* **1995**, *20*, 2532.

(5) Denk, W.; Svoboda, K. *Neuron* **1997**, *18*, 351.

(6) Köhler, R. H.; Cao, J.; Zipfel, W. R.; Webb, W. W.; Hansen, M. R. *Science* **1997**, *276*, 2039.

(7) Xu, C.; Zipfel, W. R.; Shear, J. B.; William, R. M.; Webb, W. W. *Proc. Natl. Acad. Sci. U.S.A.* **1996**, *93*, 10763.

(8) Denk, W. *Proc. Natl. Acad. Sci. U.S.A.* **1994**, *91*, 6629.

(9) Fleitz, P. A.; Brant, M. C.; Sutherland, R. L.; Strohkendl, F. P.; Larson, J. R.; Dalton, L. R. *SPIE Proc.* **1998**, *3472*, 91.

(10) He, G. S.; Bhawalkar, J. D.; Zhao, C. F.; Prasad, P. N. *Appl. Phys. Lett.* **1995**, *67*, 2433.

(11) Ehrlich, J. E.; Wu, X. L.; Lee, L.-Y.; Hu, Z.-Y.; Roedel, H.; Marder, S. R.; Perry, J. *Opt. Lett.* **1997**, *22*, 1843.

(12) Bhawalkar, J. D.; He, G. S.; Prasad, P. N. *Rep. Prog. Phys.* **1996**, *59*, 1041.

(13) (a) He, G. S.; Zhao, C. F.; Bhawalkar, J. D.; Prasad, P. N. *Appl. Phys. Lett.* **1995**, *67*, 3703. (b) Zhao, C. F.; He, G. S.; Bhawalkar, J. D.; Park, C. K.; Prasad, P. N. *Chem. Mater.* **1995**, *7*, 1979.

(14) Bhawalkar, J. D.; Kumar, N. D.; Zhao, C. F.; Prasad, P. N. *J. Clin. Med. Surg.* **1997**, *37*, 510.

(15) (a) Reinhardt, B. A.; Brott, L. L.; Clarson, S. J.; Dillard, A. G.; Bhatt, J. C.; Kannan, R.; Yuan, L.; He, G. S.; Prasad, P. N. *Chem. Mater.* **1998**, *10*, 1863. (b) Belfield, K. D.; Hagan, D. J.; Van Stryland, E. W.; Schafer, K. J.; Negres, R. A. *Org. Lett.* **1999**, *1*, 1575.

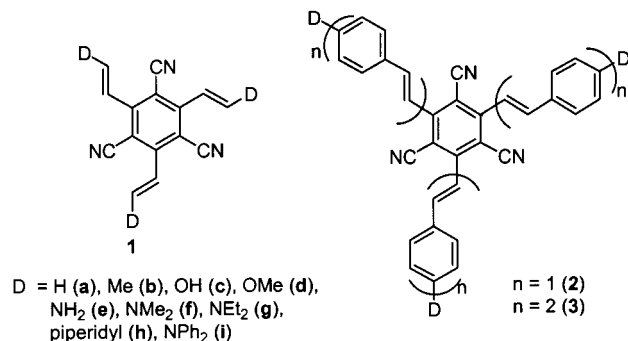
(16) Belfield, K. D.; Schafer, K. J.; Mourad, W.; Reinhardt, B. A. *J. Org. Chem.* **2000**, *65*, 4475.

(17) Kim, O.-K.; Lee, K.-S.; Woo, H. Y.; Kim, K.-S.; He, G. S.; Swiatkiewicz, J.; Prasad, P. N. *Chem. Mater.* **2000**, *12*, 284.

such effect was noted in the nonconjugated dendrimers.²¹ Macak et al. recently carried out ab initio calculations to elucidate the enhancement of the TPA cross section as a function of the number of branches, and they found that the vibronic contribution to the TPA cross section plays a crucial role in that respect.²²

Quite recently, we reported that 1,3,5-tricyano-2,4,6-tris(vinyl)benzene derivatives show significant to large first hyperpolarizabilities (β).²³ The β values of these octupolar molecules were found to be much larger than those of corresponding dipolar molecules, and these values increase as the donor strength as well as the conjugation length increase. Also, our theoretical investigation for a few series of octupolar molecules revealed that there is qualitatively a linear relationship between the β and TPA cross section and that both values increase monotonically as the donor and acceptor strengths increase.²⁴ This result strongly suggests that the derivatives of 1,3,5-tricyano-2,4,6-tris(vinyl)benzene (**2**) should also exhibit fairly large TPA cross section.

In this paper, we present the two-photon-induced fluorescence spectra of the octupolar molecules **1–3** and the TPA cross sections. A theoretical calculation on a series of molecules (**2a–2h**) will also be presented. Then, the structure–TPA



property relationship of these molecules will be established.

2. Experimental Section

Materials. 1,3,5-Tricyano-2,4,6-tris(vinyl)benzene derivatives **1–3** were available from previous study.²³ Rhodamine B and coumarine 307 were purified by repeated crystallization. HPLC grade solvents were used without further purification.

Methods. Absorption spectra were measured with a HP-8453 UV–vis system, and the fluorescence and fluorescence excitation spectra were obtained with a Amico Bowman series 2 luminescence spectrometer. The fluorescence quantum yield was determined using rhodamine B or coumarine 307 as the reference by the literature method.²⁵

(18) (a) Albota, M.; Beljonne, D.; Brédas, J.-L.; Ehrlich, J. E.; Fu, J.-Y.; Heikal, A. A.; Hess, S. E.; Kogej, T.; Levin, M. D.; Marder, S. R.; McCord-Maughon, D.; Perry, J. W.; Röckel, H.; Rumi, M.; Subramaniam, G.; Webb, W. W.; Wu, X.-L.; Xu, C. *Science* **1998**, *281*, 1653. (b) Rumi, M.; Ehrlich, J. E.; Heikal, A. A.; Perry, J. W.; Barlow, S.; Hu, Z.; McCord-Maughon, D.; Parker, T. C.; Röckel, H.; Thayumanavan, S.; Marder, S. R.; Beljonne, D.; Brédas, J.-L. *J. Am. Chem. Soc.* **2000**, *122*, 9500.

(19) Lee, W.-H.; Cho, M.; Jeon, S.-J.; Cho, B. R. *J. Phys. Chem. A* **2000**, *104*, 11033.

(20) Chung, S.-J.; Kim, K.-S.; Lin, T.-C.; He, G. S.; Swiatkiewicz, J.; Prasad, P. N. *J. Phys. Chem. B* **1999**, *103*, 10741.

(21) Adronov, A.; Fréchet, J. M.; He, G. S.; Kim, K.-S.; Chung, S.-J.; Swiatkiewicz, J.; Prasad, P. N. *Chem. Mater.* **2000**, *12*, 2838.

(22) Macak, P.; Luo, Y.; Norman, P.; Ågren, H. *J. Chem. Phys.* **2000**, *113*, 7055.

(23) Cho, B. R.; Park, S. B.; Lee, S. J.; Son, K. H.; Lee, S. H.; Lee, M.-J.; Yoo, J.; Lee, Y.-K.; Lee, K. J.; Kang, T. I.; Cho, M.; Jeon, S.-J. *J. Am. Chem. Soc.* **2001**, *123*, 6421.

(24) Lee, W.-H.; Lee, H.; Kim, J.-A.; Choi, J.-H.; Cho, M.; Jeon, S.-J.; Cho, B. R. Two-Photon Absorption and Nonlinear Optical Properties of Octupolar Molecules. *J. Am. Chem. Soc.*, in press.

(25) Demas, J. N.; Crosby, G. A. *J. Phys. Chem.* **1971**, *75*, 991.

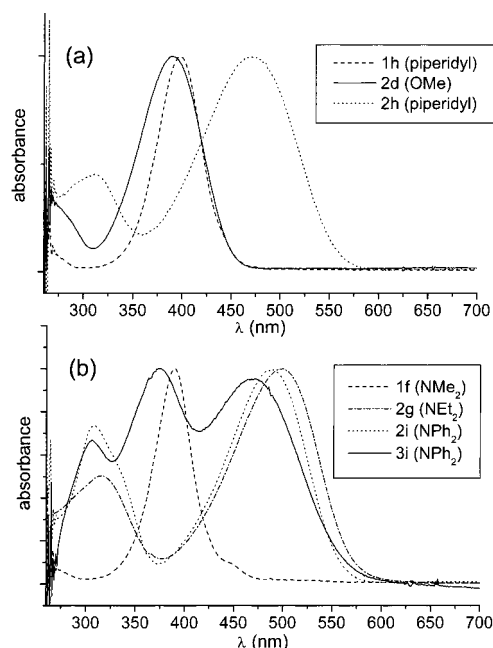


Figure 1. Absorption spectra of **1–3**.

The two-photon absorption cross section of the octupolar compounds has been measured with the two-photon-induced fluorescence method by using the nanosecond laser pulses as reported in the literature. An OPO laser (Continuum Surelite OPO, 5 ns pulses), pumped by a Q-switched Nd:YAG laser (Continuum SL-II-10), has been used as the excitation source (pulse duration \approx 5 ns, repetition rate = 10 Hz).^{18b}

Samples were dissolved in CHCl₃ at concentrations of (0.050–1.0) \times 10⁻⁴ M, and the two-photon-induced fluorescence intensity was measured. The plot of the fluorescence intensity against the sample concentration was a straight line at low concentration but showed a downward curve at higher concentration, probably because of the formation of the aggregates. The highest sample concentration determined from the linear region was used to measure the TPA cross section. The concentration of each sample employed in this study is as follows: **1f**, **1h**, and **2d**, 1.00 \times 10⁻⁴ M; **2g** and **2h**, 2.00 \times 10⁻⁵ M; **2i**, 5.00 \times 10⁻⁶ M; and **3i**, 3.00 \times 10⁻⁵ M. The TPA cross sections of **1f**, **1h**, and **2d** were measured at 780–880 nm using coumarine 307 in MeOH (1.00 \times 10⁻⁴ M) as the reference.²⁶ The excitation wavelength and reference used for **2g–i** and **3i** were 800–1050 nm and rhodamine B in methanol (1.00 \times 10⁻⁴ M), respectively.²⁶ The intensities of the two-photon-induced fluorescence spectra of the reference and sample emitted at the same excitation wavelength were determined. The TPA cross sections were calculated by using eq 1 (see Results and Discussion).

3. Results and Discussion

3A. One-Photon Absorption and Fluorescence Spectra.

Figure 1a,b shows one-photon absorption spectra of **1–3**. The absorption spectra exhibit a bathochromic shift by 104 nm as the conjugation length increases from **1f** to **2g**. However, when the conjugation length is further increased, the λ_{max} slightly decreases (compare **2i** and **3i**), probably because the structure of **3i** is significantly distorted to interrupt the effective conjugation. Also, the width of the absorption peak of **2g** is much broader than that of **1f**, indicating either that the solvent–chromophore interaction strength is larger or that the number of the one-photon-allowed excited states increases as the molecular size increases. It is interesting to note that there appear to be three peaks in the visible absorption spectrum of **3i**, whereas a series of compounds **2** exhibits only two peaks. Again, this is due to an increased number of one-photon-allowed excited

(26) Xu, C.; Webb, W. W. *J. Opt. Soc. Am. B* **1996**, *13*, 481.

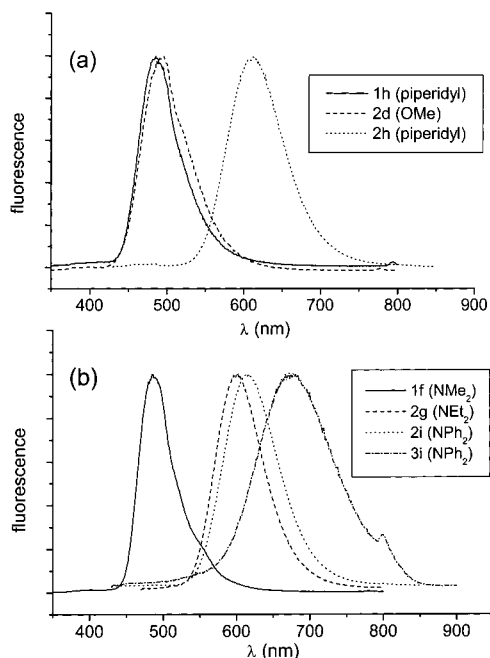


Figure 2. Steady-state fluorescence spectra of 1–3.

Table 1. Absorption and Fluorescence Maxima and Stokes Shifts of 1,3,5-Tricyano-2,4,6-tris(vinyl)benzene Derivatives^a

	1f	1h	2d	2g	2h	2i	3i
$\lambda_{\max}^{(1)}$	389	396	388	493	468	488	468
$\lambda_{\max}^{\text{fl}}$	486	485	496	602	614	614	675
$\Delta\lambda$	97	89	108	109	146	126	207

^a In nm. $\lambda_{\max}^{(1)}$ and $\lambda_{\max}^{\text{fl}}$ are the wavelengths of the maximum peak in the one-photon absorption and fluorescence spectra, respectively. $\Delta\lambda$ is the Stokes shift.

states as the conjugation length increases. For a given skeleton, the λ_{\max} values decrease with the change of the substituent in the order Et_2N (2g) > Ph_2N (2i) > piperidyl (2h) > OMe (2d). Note that the λ_{\max} of 2h appears at a shorter wavelength than those of 2g and 2i, despite its stronger electron-donating ability. This unexpected result cannot be easily explained because of a few complicating factors. First of all, the first absorption peak of the series of compounds 2 is associated with a few one-photon-allowed excited electronic states. Therefore, one cannot expect that simple monotonic behavior of the HOMO–LUMO energy gap as a function of the electron-donating strength of the substituent would be reflected by λ_{\max} . Second, the energy gap between the ground and excited electronic states is keenly dependent on the solvation energy. It is likely that the local structure of the solvation shell around each chromophore would be different for each molecule, which could be another reason for the unexpected pattern mentioned above.

The fluorescence spectra of 1–3 are displayed in Figure 2a,b. It is observed that none of these spectra have multiple peaks, which indicates that the emission occurs from the lowest excited state with the largest oscillator strength. The peak positions of the absorption and fluorescence spectra are summarized in Table 1. In contrast to the absorption spectra, the fluorescence spectra exhibit systematic bathochromic shifts with increasing conjugation length. All of the compounds show large Stokes shift ranging from 89 nm for 1h to 207 nm for 3i. As expected, the fluorescence Stokes shift increases as the conjugation length increases. Furthermore, $\lambda_{\max}^{\text{fl}}$ monotonically increases as the donor strength increases (OMe (2d) \approx Et_2N (2g) < piperidyl (2h)). This means that the energy gap between the ground and

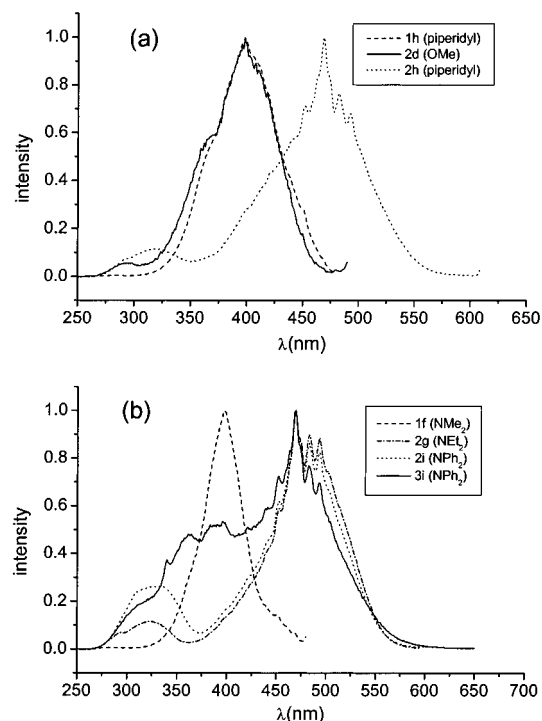


Figure 3. Single-photon excitation spectra of 1–3.

lowest excited states decreases monotonically as the charge-transfer extent of the electronic ground state increases. Note that the electronic structure of the excited electronic state of these octupolar molecules is close to the charge-transfer structure. Therefore, as the donor strength increases, the charge-transfer character of the excited electronic state would increase, and consequently, the solvation energy of the excited electronic state becomes large, and the fluorescence Stokes shift will increase, too. This pattern is clearly observed experimentally (see Table 1).

3B. Single-Photon Excitation Spectra. Figure 3a,b shows the excitation spectra of 1–3 in CHCl_3 solutions with a spectral resolution of ~ 0.5 nm. The excitation wavelength was varied from 250 to 700 nm, and the emission at 500 (1f, 1h, 2g) or 600 nm (2h, 2i, 3i) was monitored as a function of the excitation wavelength. For instance, the spectrum in Figure 3b of 2g shows four peaks centered at 485 nm and an additional broad peak at 325 nm. Although the positions of these two broad peaks are similar to those observed in the absorption spectrum (see Figure 1b), the band shapes are different. Particularly, there appear relatively sharp features near the absorption maximum wavelength. If the internal conversion efficiencies of all excited states are identical, the single-photon excitation spectrum merely reflects the initial absorption probability, which is nothing but the information gained from the absorption spectrum. However, the observed difference between the absorption spectrum and the single-photon excitation spectrum is critical evidence that the internal conversion efficiencies of excited states are different from one another. This also suggests that more than one excited state is involved in the absorption process to create the broad band at the absorption maximum. Typically, the electronic internal conversion from one excited state to the lowest excited state occurs at the curve-crossing region, and its intensity is related to the Franck–Condon (FC) factors.²⁷ The more different the molecular structures of two electronic states are, the smaller the magnitudes of the FC factors are. Therefore, the larger the

(27) Atkins, P. W. *Physical Chemistry*, 6th edition; Oxford University Press: Oxford, 1998.

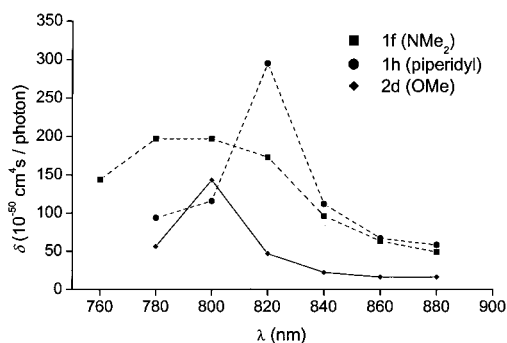


Figure 4. Two-photon-induced fluorescence spectra of **1–3**.

difference between the absorption and single-photon excitation spectra is, the more significantly different the molecular structures of the electronic excited states are. Comparison of the single-photon excitation and absorption spectra for **1–3** reveals that the difference between them is significant as the conjugation length increases. This trend coincides with the Stokes shift observed for this series of octupoles. This relationship is an indication that both the magnitudes of the Stokes shifts and the differences between the single-photon excitation and absorption spectra arise from the structural changes of the octupoles that occur upon excitation from the ground state.

3C. Two-Photon Fluorescence Spectra and Two-Photon Absorption Coefficients. The two-photon cross section δ was measured by using the two-photon-induced fluorescence measurement technique with the following equation

$$\delta = \frac{S_s \Phi_r \phi_r c_r}{S_r \Phi_s \phi_s c_s} \delta_r \quad (1)$$

where the subscripts s and r stand for the sample and reference molecules.^{18b} The intensity of the signal collected by a PMT detector is denoted as S . Φ is the fluorescence quantum yield. ϕ is the overall fluorescence collection efficiency of the experimental apparatus. The number density of the molecules in solution is denoted as c . δ_r is the TPA cross section of the reference molecule.

As can be seen in Figure 4, the two-photon-induced fluorescence excitation spectra for **1–3** are quite similar to the single-photon absorption spectra shown in Figure 1, except that the wavelength is doubled. Unlike the quadrupolar molecule having an inversion center, this result shows that one- and two-photon-allowed states of these octupolar compounds are more or less the same.

Table 2 summarizes the wavelengths of the single- and two-photon absorption maxima ($\lambda_{\max}^{(1)}$ and $\lambda_{\max}^{(2)}$), $\beta(0)$, and the maximum values of the two-photon absorption cross section (δ_{\max}). For all compounds, $\lambda_{\max}^{(2)}$ appeared either at twice the wavelength of the maximum peak ($2\lambda_{\max}^{(1)}$) or where there are strong bands in the excitation spectra because the one- and two-photon-allowed states are the same. This aspect is in contrast with the linear quadrupolar molecule where the TPA state is not identical to the one-photon-allowed state because of the molecular symmetry. The δ_{\max} value increases as the donor strength and the conjugation length increase. As has been shown previously, a stronger donor would not only increase the ground-state charge-transfer character to further increase the TPA transition matrix element but also decrease the energy gap between the ground and first excited state as found in the monotonic red shift of the peak frequency of the fluorescence spectrum. Also, both the charge-transfer character as well as

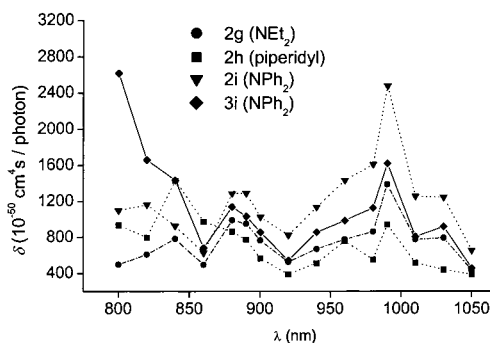


Table 2. Nonlinear Optical and Two Photon Absorption Properties of 1,3,5-Tricyano-2,4,6-tris(vinyl)benzene Derivatives^a

	$\lambda_{\max}^{(1)}$	$\lambda_{\max}^{(2)}$	$\beta_{\text{exp}}(0)$	$\beta_{\text{cal}}(0)$	BLA (Å)	Φ	δ_{\max}	$\delta_{\max}^{\text{cal}}$
1f	389	800	25	15		0.0178	197	
1h	396	820	17	17		0.0165	295	
2a		(581)		7.2	−0.144 75			1099
2b		(595)		10	−0.142 80			1257
2c		(612)		13	−0.141 60			1791
2d	388	800	14	15	−0.141 30	0.003 29	143	2105
		(620)						
2e		(635)		22	−0.136 54			1948
2f		(654)		29	−0.135 90			2278
2g	493	990	65	32	−0.135 35	0.112	1390	2362
		(663)						
2h	468	840	69	33	−0.132 50	0.0662	1430	2648
		(658)						
2i	488	990	124			0.246	2480	
3i	468	800	107			0.0325	2620	

^a $\lambda_{\max}^{(1)}$ and $\lambda_{\max}^{(2)}$ are the wavelengths of the maximum peaks in the one-photon and two-photon-absorption spectra in nm, respectively. The numbers in the parentheses are the calculated $\lambda_{\max}^{(2)}$ values. The $\beta(0)$ value is in 10^{-30} esu.²³ BLA is the bond length alternation. Φ is quantum yield. The unit of the TPA cross section is 10^{-50} cm⁴ s/photon. δ_{\max} is the peak TPA cross section when the TP-induced fluorescence method is used, whereas $\delta_{\max}^{\text{cal}}$ is the theoretically calculated TPA cross section when the TP absorption is assumed to be directly measured. Thus, it should be noted that the experimental δ_{\max} and theoretically calculated $\delta_{\max}^{\text{cal}}$ assume two different detection methods.

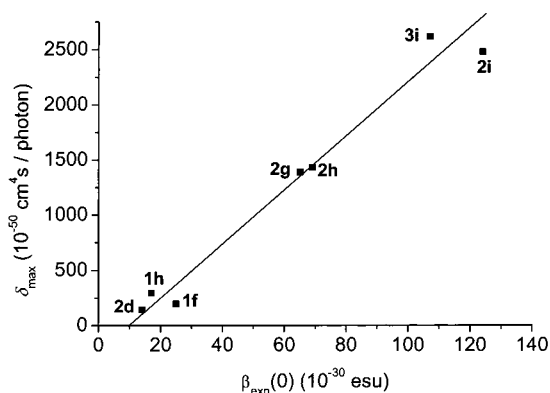


Figure 5. Plot of δ_{\max} vs $\beta_{\text{exp}}(0)$.

the electronic transition frequency are expected to increase as the conjugation length increases. A combination of these effects would be to increase the δ_{\max} , as observed. In addition, the values of $\delta_{\max} = 2480$ and 2620 GM (GM = 10^{-50} cm⁴s/photon) determined for **2i** and **3i** are comparable to those of recently reported chromophores with the largest TPA cross sections.¹⁸

The plot of δ_{\max} versus $\beta(0)$ for **1–3** is depicted in Figure 5. The two quantities are almost linearly proportional to each other. Although the two properties are associated with different optical

nonlinearities, that is, $\beta(0)$ is the zero-frequency-limit of the second-order molecular susceptibility, whereas δ is the imaginary part of the third-order one, the linear relationship between the two is believed to be a crucial guideline for the synthetic design strategy to maximize the TPA cross section of the octupolar molecule. This relationship was theoretically predicted by using the simple four-state valence-bond three-charge-transfer model in ref 28 and confirmed by comparing the ab initio calculated β and δ for a few series of octupolar molecules.²⁴ However, there did not exist any real experimental data to test this linear relationship before. Qualitatively speaking, both δ and β are increasing functions with respect to the charge-transfer character, which is in turn determined by the electron-donating ability of the substituted chemical group. Thus, the relationship seems reasonable, but there is now concrete evidence that the two quantities should be correlated with each other as discussed in this paper.

It is also interesting to note that both δ_{\max} and β increase dramatically upon replacing diethylamino groups in **2g** with diphenylamino groups (**2i**). The result could be explained by noting that (i) NPh_2 has a better cation stabilizing ability and (ii) the additional degree of spatial delocalization of the mobile electrons for **2i** is possible. To elaborate point (i), it should be noted that the diphenylamino group is a much weaker electron donor than the former, as indicated by the smaller $\text{p}K_a$ value of Ph_2NH (0.9) than Et_2NH (10.8) and by the more positive oxidation potential reported for 4,4'-bis(diphenylamino)stilbene than the corresponding dibutylamino derivative.^{18b,29} Hence, the ground state of **2i** would be located at slightly lower energy than **2g**. On the other hand, a larger stabilization of the first excited state would be provided by the diphenylamino group, into which the positive charge can be stabilized. Consequently, the energy gap between the ground and the first excited state would be decreased. Consistent with this interpretation is the larger Stokes shift observed for **2i** (Table 1). This would enhance the intramolecular charge transfer from the donor to the cyano groups to increase both β and δ_{\max} . Finally, the values of δ_{990} , TPA cross sections measured at 990 nm, for **2i** and **3i** are 2480 and 1620 GM, respectively (Figure 4). Also, the $\beta(0)$ values for **2i** and **3i** are 124×10^{-30} esu and 107×10^{-30} esu, respectively (Table 2). The smaller values of δ_{990} and $\beta(0)$ for **3i** are probably due to the distorted structure of **3i**, which may have nullified this special effect (vide supra). In summary, **2g–i** and **3i** not only show unusually large TPA cross sections but also emit strong two-photon-induced fluorescence, and these two properties are important requirements for practical applications.

3D. Theoretical Calculations of the TPA Spectra. In this subsection, we will present a series of semiempirical calculation results for compounds **2**. First of all, let us consider the first hyperpolarizability given as

$$\tilde{\beta} = \sum_{m \neq g} \sum_{n \neq g} \frac{\mu_{gm} \bar{\mu}_{mn} \mu_{ng}}{(E_m - E_g)(E_n - E_g)} \quad (2)$$

where the transition dipole matrix element between $|m\rangle$ and $|n\rangle$ was denoted as μ_{mn} and $\bar{\mu}_{mn} \equiv \mu_{mn} - \mu_{gg} = \mu_{mn}$. Here, μ_{gg} is the permanent dipole moment of the ground electronic state, and it vanishes for the octupolar molecules because of the molecular symmetry. Instead of the above SOS (sum-over-states) expression, the finite-field method with the AM1 Hamiltonian

(28) (a) Lee, Y.-K.; Jeon, S.-J.; Cho, M. *J. Am. Chem. Soc.* **1998**, *120*, 10921. (b) Lee, H.; An, S.-Y.; Cho, M. *J. Phys. Chem. B* **1999**, *103*, 4992.

(29) Dean, J. A. *Handbook of Organic Chemistry*; McGraw-Hill: New York, 1987, p 8–25.

is used to calculate β for the eight compounds, **2a–h**. However, the geometry optimization was performed by using the Gaussian 98 program with the basis set of 6-31G.³⁰ To make direct comparisons of the AM1-calculated β with the experimental values, the orientationally averaged quantity, $\beta_{\text{cal}}(0) = \langle \beta_{\text{ZZZ}}^2 \rangle^{1/2} = \sqrt{24\beta_{\text{ZZZ}}^2/105}$, where β_{ZZZ} is the [ZZZ] tensor element with the molecular z -axis being one of the C_2 rotation axes, should be obtained (see Table 2).³¹ Although the calculated values, $\beta_{\text{cal}}(0)$, are quantitatively a bit different from the experimental data, the general trend of increasing β with respect to the donor strength is in an excellent agreement with the experiment. As the donor strength increases from H to piperidyl group, the bond length alternation (BLA), which is defined as the difference between the C=C bond length of the vinyl group and average bond length of the two C–C bonds connected to the vinyl C=C bond, increases. Therefore, the BLA– β (relationship studied before is also found to be valid for the series of compounds **2a–h**, that is to say, β is a monotonically increasing function of the BLA for the planar octupolar molecules.

Next, we shall present the semiempirical calculation results of the TPA cross section. The TPA spectrum can be calculated by using the following equation

$$\delta(\omega) = \frac{4\pi^3 a_0 \alpha \omega^2 L^4}{15c_0 \eta^2} \sum_f \sigma_{fg}(\omega) \frac{\gamma_{fg}/\pi}{(\omega - \omega_{fg})^2 + \gamma_{fg}^2} \quad (3)$$

where a_0 , α , c_0 , and η are the Bohr's radius, fine structure constant, speed of light, and refractive index of the solvent at ω , respectively. The local field correction factor, L , is given as $L = 3\eta^2/(2\eta^2 + 1)$. In eq 3, the TP transition probability from $|g\rangle$ to $|f\rangle$ was denoted as $\sigma_{fg}(\omega)$

$$\sigma_{fg}(\omega) = 2 \sum_{\alpha\beta} \{ \mathbf{\Gamma}_{\alpha\alpha}(\omega) \mathbf{\Gamma}_{\beta\beta}^*(\omega) + 2 \mathbf{\Gamma}_{\alpha\beta}(\omega) \mathbf{\Gamma}_{\alpha\beta}^*(\omega) \} \quad (4)$$

where the TP transition amplitude tensor, $\mathbf{\Gamma}$, is

$$\mathbf{\Gamma}_{\alpha\beta}(\omega) = \sum_i \left\{ \frac{\mu_{fi}^\alpha \mu_{ig}^\beta}{\omega - (E_i - E_g)/\hbar} + \frac{\mu_{fi}^\beta \mu_{ig}^\alpha}{\omega - (E_i - E_g)/\hbar} \right\} \quad (5)$$

Because of the molecular symmetry of the planar octupolar molecules, the tensor elements of $\mathbf{\Gamma}$ satisfy the following relationship

$$|\mathbf{\Gamma}_{zz}(\omega)| = |\mathbf{\Gamma}_{xx}(\omega)| \quad (6)$$

where the molecular x -axis is perpendicular to the molecular z -axis and is on the molecular plane. The electronic dephasing constant of the $|f\rangle$ -state is γ_{fg} , and its magnitude is difficult to estimate experimentally. Throughout this section, it is assumed to be 0.13 eV for all molecules **2a–h**.³² In fact, the

(30) Frisch, M. J.; Trucks, G. W.; Schlegel, H. B.; Scuseria, G. E.; Robb, M. A.; Cheeseman, J. R.; Zakrzewski, V. G.; Montgomery, J. A., Jr.; Stratmann, R. E.; Burant, J. C.; Dapprich, S.; Millam, J. M.; Daniels, A. D.; Kudin, K. N.; Strain, M. C.; Farkas, O.; Tomasi, J.; Barone, V.; Cossi, M.; Cammi, R.; Mennucci, B.; Pomelli, C.; Adamo, C.; Clifford, S.; Ochterski, J.; Petersson, G. A.; Ayala, P. Y.; Cui, Q.; Morokuma, K.; Malick, D. K.; Rabuck, A. D.; Raghavachari, K.; Foresman, J. B.; Cioslowski, J.; Ortiz, J. V.; Stefanov, B. B.; Liu, G.; Liashenko, A.; Piskorz, P.; Komaromi, I.; Gomperts, R.; Martin, R. L.; Fox, D. J.; Keith, T.; Al-Laham, M. A.; Peng, C. Y.; Nanayakkara, A.; Gonzalez, C.; Challacombe, M.; Gill, P. M. W.; Johnson, B. G.; Chen, W.; Wong, M. W.; Andres, J. L.; Head-Gordon, M.; Replogle, E. S.; Pople, J. A. *Gaussian 98*; Gaussian, Inc.: Pittsburgh, PA, 1998.

(31) Hendrickx, E.; Clays, K.; Persoons, A. *Acc. Chem. Res.* **1998**, *31*, 675.

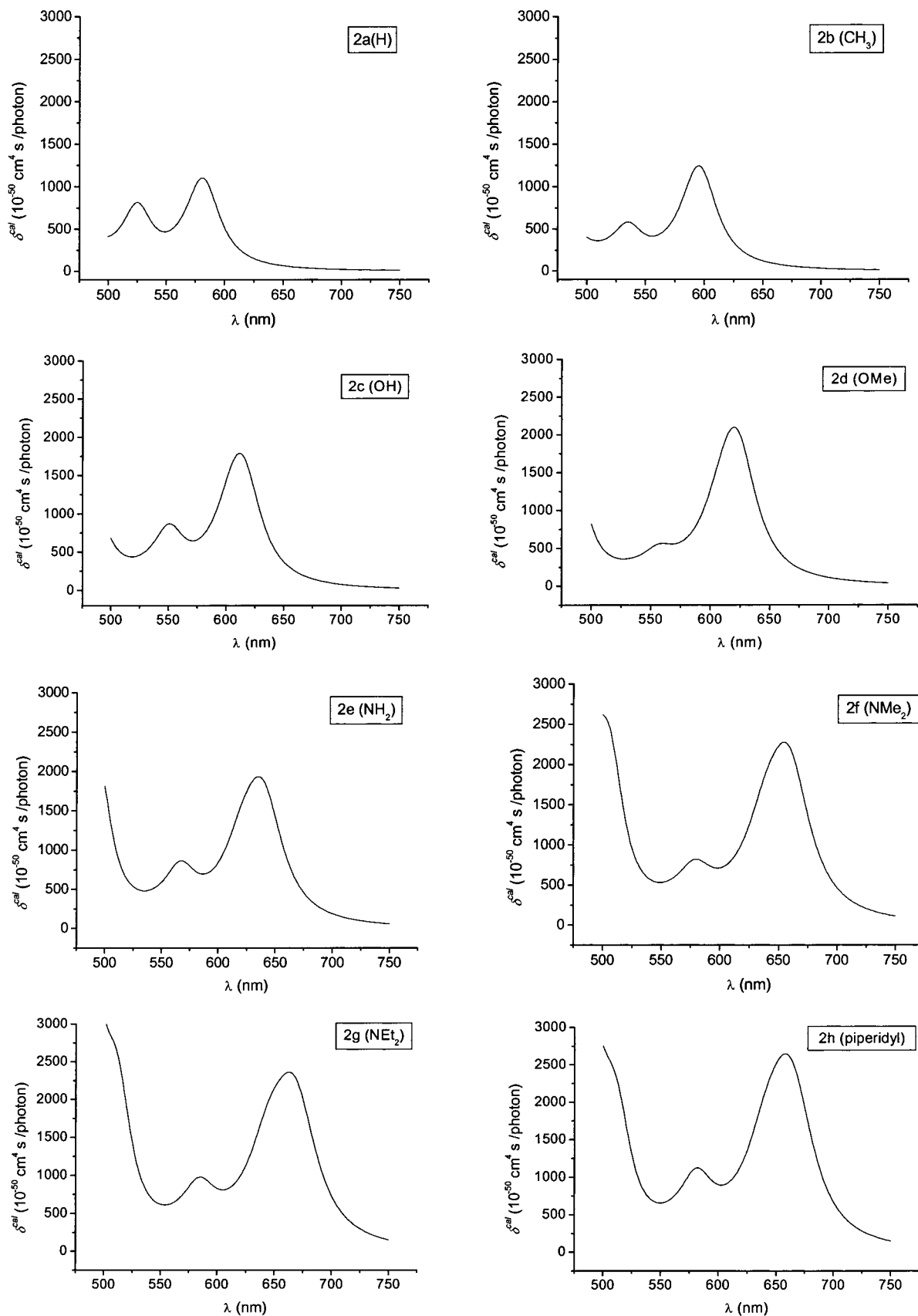


Figure 6. Theoretically calculated TPA spectra of **2a–h**.

required dephasing constants are different for different TPA states, so one has to put in correct γ_{fg} values for different $|f\rangle$ -states. However, these data are not experimentally available and cannot be simply estimated from the absorption spectra. Nevertheless, the value, 0.13 eV, is found to be reasonable

on the basis of the comparison between the theoretically calculated TPA spectra and TP-induced fluorescence spectra. The units of $\delta(\omega)$ will become $10^{-50} \text{ cm}^4 \text{ s photon}^{-1}$, if cgs units are used for a_0 and c_0 and atomic units are used for $\sigma_{fg}(\omega)$, ω , and γ_{fg} .

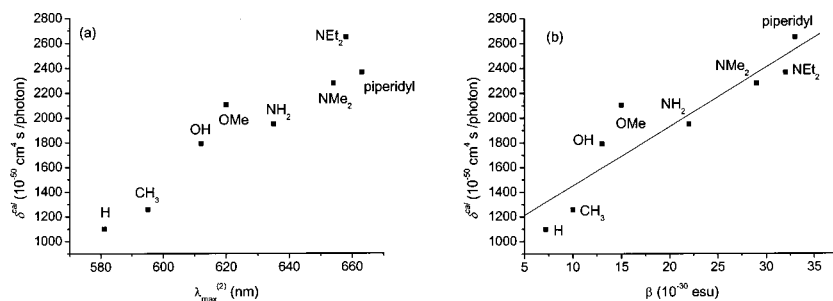


Figure 7. (a) Theoretically calculated $\delta_{\max}^{\text{cal}}$ vs $\lambda_{\max}^{(2)}$. (b) Theoretically calculated $\delta_{\max}^{\text{cal}}$ vs $\beta_{\text{cal}}(0)$.

To calculate the TPA cross section, $\delta(\omega)$, the TPA transition amplitude, $\Gamma_{\alpha\beta}(\omega)$, in eq 5 should be estimated by carrying out the sum-over-state (SOS) calculation. In this paper, 10 excited electronic states will be considered for the SOS calculation. The transition dipole matrix elements and energies of 10 excited states were calculated by using the INDO-SDCI method.³³ Although one might have to include a large number of excited states to obtain an accurate $\Gamma_{\alpha\beta}(\omega)$ value, it is believed that the general trend of δ with respect to the structural variation induced by the electron-donating group can be successfully described by the numerical calculation outlined above. Furthermore, it was confirmed that only a few low-lying excited states strongly contribute to the TPA process of these octupolar molecules.

It is now necessary to make a quantitative comparison with the experimental results. Noting that the first TPA peak is given by a sum of the contributions from a few TPA excited electronic states, one should not make a comparison of the experimentally measured δ_{\max} presented in Table 2 with the semiempirically calculated $\delta_{\max}^{\text{cal}}$ value with the lowest excited state contribution only. Thus, we first numerically calculate the TPA spectra with eq 3 with all parameters obtained from the INDO-SDCI calculations. In Figure 6, the numerically calculated TPA spectra for **2a–h** are plotted. Here, it should be noted that because of the ignorance of the solvation by liquid chloroform the center wavelength of the TPA peak is about 200 nm blue shifted in comparison to that of the experimentally measured TPA spectrum (compare Figure 6 with Figure 4). Other than this obvious discrepancy, however, the existence of the second peak at the smaller wavelength region is well reproduced by the present calculation. The numerically estimated $\delta_{\max}^{\text{cal}}$ values, from Figure 6, are summarized in Table 2 (see the last column). Overall, the order of magnitude of $\delta_{\max}^{\text{cal}}$ is similar to those of the TP-induced fluorescence experiment. Furthermore, the increasing pattern of $\delta_{\max}^{\text{cal}}$ with respect to the donor strength is clearly observed in the present calculation. In Figure 7a, $\delta_{\max}^{\text{cal}}$ is plotted with respect to the wavelength at the maximum TPA cross section. As the donor strength increases, $\lambda_{\max}^{(2)}$, estimated from the theoretically calculated TPA spectra in Figure 6, increases, and the TPA cross section also increases. This trend can be easily understood by noting that the role of the electron-donating group is to make the extent of the π -electron delocalization over the entire molecule large, which further makes the transition dipole matrix elements between the ground electronic state and the TPA excited states increase. Combining

(32) Although in refs 18 and 22 the electronic dephasing constant was assumed to be 0.1 eV, we found that the value 0.13 eV seems reasonable for the series of octupolar molecules considered in this paper. Nevertheless, the general trend found in this paper does not strongly depend on the absolute magnitude of γ_{fe} .

(33) ZINDO program; Molecular Simulations, Inc.: San Diego, CA, 1997.

these effects together, one can explain why the TPA cross section increases as the charge-transfer character, represented by the BLA, increases.

We next compare the finite-field-calculated β and TPA cross section $\delta_{\max}^{\text{cal}}$ for the series of compounds **2a–h**. In ref 24, four representative series of octupolar molecules, such as triphenylmethane dyes and triphenylamine derivatives, were considered as the prototype octupolar molecules for the investigation of the β – δ_{\max} relationship. There, on the basis of the effective four-state model, it was found that the two quantities β and δ_{\max} are linearly proportional to each other. This relationship was confirmed by directly comparing the ab initio calculated values. In this paper, we also confirmed this relationship experimentally in section 3C; note that, for compounds **2d–h**, the increasing pattern of β is similar to that of δ_{\max} . Again, for the series of compounds **2a–h**, the semiempirically calculated $\delta_{\max}^{\text{cal}}$ values are plotted with respect to the AM1-calculated β in Figure 7b. The linear relationship is also found for these octupolar molecules.

4. Summary

In this paper, the TPA properties of planar octupolar molecules have been investigated both experimentally and theoretically. The linear and nonlinear optical properties were also studied in detail. Overall, the effects of the conjugation length and substituted electron donor strength on the absorption, fluorescence, single-photon excitation detected by measuring fluorescence intensity, and TPA cross section were investigated in detail. Furthermore, the linear relationship between the first hyperpolarizability and the TPA cross section of a few series of octupolar molecules (**1–3**) was confirmed experimentally with additional supporting evidence from the semiempirical calculation. Perhaps, one of the most crucial conclusions of the present paper is that the octupolar molecule can serve as an alternative TPA dye for a variety of applications mentioned in section 1. Although a number of push–pull polyenes and linear quadrupolar molecules have been synthesized, used, and extensively studied because of their large TPA cross sections as well as the possibility of replacing previously known TPA dyes, here an additional structural motif based on the C_3 -symmetrical molecular geometry was suggested and would be a promising direction for further development of novel TPA dyes.

Acknowledgment. This work was supported by a National Research Laboratory grant from MOST and CRM-KOSEF. M.C. is grateful for the support from KISTEP via the Creative Research Initiatives Program (MOST). S.H.L., Y.-S.S., Y.K.L., and H.L. were supported by BK21 scholarship.